

# Flip Chip Bonding of $68 \times 68$ MWIR LED Arrays

Naresh Chandra Das, *Senior Member, IEEE*, Mónica Taysing-Lara, Kimberley Anderson Olver, Fouad Kiamilev, J. P. Prineas, J. T. Olesberg, E. J. Koerperick, L. M. Murray, and Tom F. Boggess

**Abstract**—The flip chip bonding process is optimized by varying the bonding pressure, temperature, and time. The  $68 \times 68$  mid wave infrared (MWIR) LED array was hybridized onto Si-CMOS driver array with same number of pixels. Each pixel has two indium bumps, one for cathode and another for anode. Both LED array and CMOS drivers have  $15\text{-}\mu\text{m}$ -square indium bump contact pads. We used Karl Suss FC150 flip chip machine for bonding of CMOS driver array onto LED array. From the LED current–voltage characteristics, it is concluded that the optimized flip chip bonding process results in uniform contact and very low contact resistance. Both electrical and optical characteristics of LED array after flip chip bonding are presented.

**Index Terms**—CMOS drivers, contact resistance, flip chip bonding, led array.

## I. INTRODUCTION

PASSIVE IR imaging and IR detector arrays for seekers play a very important role in missile defense operations and systems as well as for other DOD applications. The seeker testing requires large 2-D arrays, high frame rates, and large dynamic range IR sources. Several IR sources have been integrated into the hardware in the loop (HWIL) facility in the past, including a scanning laser array, resistive array, and digital micro mirror devices (DMD) [1]. We have shown in an earlier publication that mid-wave infrared (MWIR) light-emitting diodes (LED) can be used for IR scene generation [2]. MWIR light sources are of growing importance because of applications in infrared scene generation, infrared counter measures (IRCM), spectroscopic chemical and biological threat monitoring, medical diagnostics, and gas sensors.

MWIR LEDs are desirable for many such applications because of considerable advantages in terms of low cost, small volume, long-term reliability, broad spectral content,

and fast switching speed. For MWIR region ( $3\text{--}5\ \mu\text{m}$  emission wavelength) GaSb-based substrate material is preferred. The transmission of IR light through GaSb material varies between 5%–30% and depends on the type of substrate dopants (n- or p-type). Hence, for bottom emitting LED devices, it is desirable to remove the bulk of the GaSb substrate material to acquire sufficient light from the device active region.

For IR scene generation applications, the LED devices are required to simulate very high temperature targets on the order of 3000 K apparent black body temperature. Hence, the goal is to fabricate LED devices maximizing light output for a particular epitaxial design structure. Heat dissipation is also another important factor in designing an MWIR LED array. One possible method to achieve low contact resistance and good thermal conductivity is to use flip chip technology [3]–[5]. Flip chip hybridization is a packaging technique whereby a chip is attached to a substrate facedown eliminating peripheral wire bonding. A grid of solder bumps on the surface of the active area of the die is joined directly to a corresponding set of solder bumps on the substrate. This will shorten the thermal path between the active light emitting region of LEDs and heat sink. Flip chip bonding of IR detectors with readout integrated circuits has been extensively reported [6], [7]. High (force) pressure thermal compression [8] as well as low (force) pressures bonding with solder reflow with epoxy underfill [9] are used for flip chip bonding. However, very few published reports are available on flip chip bonding of LEDs to CMOS read-in integrated driver circuits [10]. Unlike single indium bump on silicon readout circuit in [3], we used two bumps, one on readout array side and other on LED array side. In this paper, we report our experimental findings of a detailed optimization procedure for flip chip bonding of  $68 \times 68$  MWIR LED arrays onto Si-CMOS driver arrays. Optical and electrical properties of the fabricated LED array will also be reported.

## II. EXPERIMENTAL

For this experiment, we used super lattice light-emitting diode (SLED) structure, consists of 16 cascaded MWIR super lattice emission regions ( $8.9/16$  monolayer's (ml) InAs/GaSb) separated by (n InAs/GaSb super lattice grade)/(p+ GaSb) tunnel junctions. Graded super lattices were introduced between the GaSb clads and the first and last MWIR super lattice emission regions in order to smooth out interfacial spikes in the real space band structure. The structure was capped with a thin layer of p++ type GaSb, which has favorable band offsets for Ohmic p-contacts, blocks electrons from reaching the semiconductor-air surface, and is nominally transparent for reflection of emitted light off the top contact.

Device fabrication started with inductively coupled plasma (ICP) dry etching to define the mesa area. The square mesa size

Manuscript received March 31, 2008; revised July 28, 2008. Current version published January 08, 2009. This work was supported by the T&E/S&T Program through the University of Iowa under Contract W91ZLK-06-C-0006. This work was recommended for publication by Associate Editor E. Perfecto upon evaluation of the reviewers comments.

N. C. Das and M. Taysing-Lara are with the Microphotonics Branch, Army Research Laboratory, Adelphi, MD 20783 USA (e-mail: ndas@arl.army.mil; tysingl@arl.army.mil).

K. A. Olver is with the EO/IR Materials and Devices Branch, Army Research Laboratory, Adelphi, MD 20783 USA (e-mail: kolver@us.army.mil).

F. Kiamilev is with the Electrical Engineering Department, University of Delaware, DE 19716 USA (e-mail: kiamilev@att.net).

J. P. Prineas, J. T. Olesberg, E. J. Koerperick, L. M. Murray, and T. F. Boggess are with Physics Department, University of Iowa, Iowa City, IA 52242 USA (e-mail: preneas@uiowa.edu; olesberg@uiowa.edu; Koerperick@uiowa.edu; Murray@uiowa.edu; thomas-boggess@uiowa.edu).

Color versions of one or more of the figures in this paper are available online at <http://ieeexplore.ieee.org>.

Digital Object Identifier 10.1109/TEPM.2008.2005062

# Report Documentation Page

Form Approved  
OMB No. 0704-0188

Public reporting burden for the collection of information is estimated to average 1 hour per response, including the time for reviewing instructions, searching existing data sources, gathering and maintaining the data needed, and completing and reviewing the collection of information. Send comments regarding this burden estimate or any other aspect of this collection of information, including suggestions for reducing this burden, to Washington Headquarters Services, Directorate for Information Operations and Reports, 1215 Jefferson Davis Highway, Suite 1204, Arlington VA 22202-4302. Respondents should be aware that notwithstanding any other provision of law, no person shall be subject to a penalty for failing to comply with a collection of information if it does not display a currently valid OMB control number.

|   |                                    |                                     |                            |   |                                 |
|---|------------------------------------|-------------------------------------|----------------------------|---|---------------------------------|
| 1. REPORT DATE<br><b>28 JUL 2008</b>  |                                    | 2. REPORT TYPE                      |                            | 3. DATES COVERED<br><b>00-00-2008 to 00-00-2008</b> |                                 |
| 4. TITLE AND SUBTITLE<br><b>Flip Chip Bonding of 68 x 68 MWIR LED Arrays</b>  |                                    |                                     |                            | 5a. CONTRACT NUMBER                                 |                                 |
|   |                                    |                                     |                            | 5b. GRANT NUMBER                                    |                                 |
|   |                                    |                                     |                            | 5c. PROGRAM ELEMENT NUMBER                          |                                 |
| 6. AUTHOR(S)  |                                    |                                     |                            | 5d. PROJECT NUMBER                                  |                                 |
|   |                                    |                                     |                            | 5e. TASK NUMBER                                     |                                 |
|   |                                    |                                     |                            | 5f. WORK UNIT NUMBER                                |                                 |
| 7. PERFORMING ORGANIZATION NAME(S) AND ADDRESS(ES)<br><b>University of Delaware, Department of Electrical and Computer Engineering, Newark, DE, 19716</b> |                                    |                                     |                            | 8. PERFORMING ORGANIZATION REPORT NUMBER            |                                 |
| 9. SPONSORING/MONITORING AGENCY NAME(S) AND ADDRESS(ES)   |                                    |                                     |                            | 10. SPONSOR/MONITOR'S ACRONYM(S)                    |                                 |
|   |                                    |                                     |                            | 11. SPONSOR/MONITOR'S REPORT NUMBER(S)              |                                 |
| 12. DISTRIBUTION/AVAILABILITY STATEMENT<br><b>Approved for public release; distribution unlimited</b>   |                                    |                                     |                            |   |                                 |
| 13. SUPPLEMENTARY NOTES   |                                    |                                     |                            |   |                                 |
| 14. ABSTRACT<br><b>see report</b>   |                                    |                                     |                            |   |                                 |
| 15. SUBJECT TERMS   |                                    |                                     |                            |   |                                 |
| 16. SECURITY CLASSIFICATION OF:   |                                    |                                     | 17. LIMITATION OF ABSTRACT | 18. NUMBER OF PAGES                                 | 19a. NAME OF RESPONSIBLE PERSON |
| a. REPORT<br><b>unclassified</b>  | b. ABSTRACT<br><b>unclassified</b> | c. THIS PAGE<br><b>unclassified</b> |                            |   |                                 |

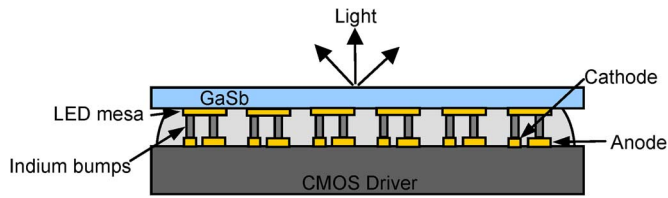


Fig. 1. Schematic cross-sectional view of the LED array.

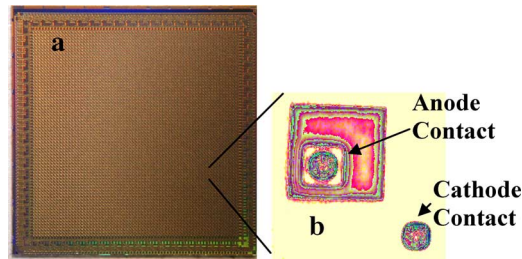


Fig. 2. (a) CMOS driver array and (b) single driver pixel.

was  $75\ \mu\text{m}$ . The etch depth for mesa isolation was  $3.0\ \mu\text{m}$ . A silicon nitride layer of  $3000\ \text{\AA}$  was then deposited by plasma-enhanced chemical vapor deposition (PECVD) technique. Contact windows were opened in the  $\text{Si}_3\text{N}_4$ . A contact Ti/Au metallization was done by electron beam evaporation for both the top and bottom contacts. A chromium/indium vacuum-thermal evaporation was the last photolithography step. A  $300\ \text{\AA}$  of chromium immediately followed by  $5\ \mu\text{m}$  of indium was deposited on the LED arrays. The resulting deposition gave indium solder bumps  $5\ \mu\text{m}$  in height by  $15\ \mu\text{m}$  square. Two indium bumps per pixel, one on the cathode and the other on the anode were deposited. The total number of indium solder bumps for each  $68 \times 68$  LED array was 9248. The same procedure was used to place indium bumps on the CMOS drivers. An LED device was then flip chip bonded to a corresponding CMOS driver, epoxy under filled, and the GaSb bulk substrate then removed. The  $68 \times 68$  LED array has  $8.4\ \text{mm}^2$  square area. Fig. 1 shows a schematic cross-sectional view of the flip chip mount LED array.

After flip chip bonding of LED array onto CMOS array, we removed the bottom GaSb substrate material by lapping and the light emission is observed through the substrate side [11]. We measured device IV characteristics before and after lapping. The IV characteristics do not change with lapping the substrate as both the anode and cathode contacts are on the top surface.

The size of the  $68 \times 68$  CMOS driver array (Fig. 2) is  $9.5\ \text{mm}^2$ . The driver array was fabricated in the 130-nm IBM 8HP SiGe process. Although the 8HP process is suited for high speed designs, this process was ultimately chosen for the high current densities afforded by the copper interconnect layers. The unit cells were designed to source up to 100 mA to the LED, be individually addressable, and have analog drive and memory that can operate at a 1-kHz array refresh rate. Each unit cell contains a CMOS logic switch, a capacitor, and a SiGe HBT driver. The switch is controlled by row and column select lines, which when activated charges the capacitor. The voltage stored on the capacitor controls the output current from the driver to the LED. Each unit cell [Fig. 2(b)] contains a CMOS logic switch, a capacitor, and a SiGe HBT driver. The cells have

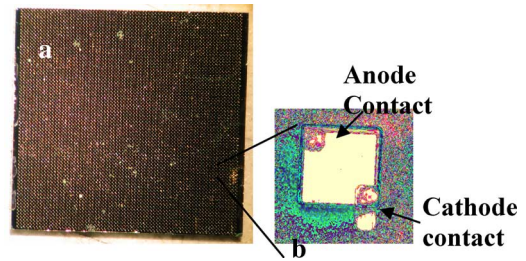


Fig. 3. (a) Photograph of  $68 \times 68$  LED array and (b) single pixel LED.

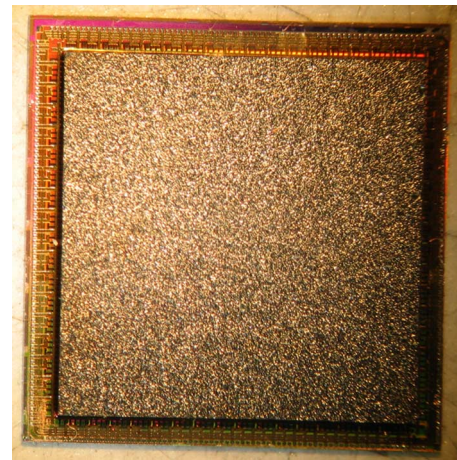


Fig. 4. Photograph of LED array flip chip mounted on to the CMOS drive array.

a  $120\text{-}\mu\text{m}$  pitch and contain two  $15\text{-}\mu\text{m}$ -square pad openings for the anode and cathode contacts to the LED. The CMOS switch in each cell enables individual addressability of the LED driver array. The switch is controlled by row and column select lines, which when activated charges the storage capacitor to a variable input voltage.

Pictures of the ( $68 \times 68$ ) LED array and single pixel LED are shown in Fig. 3. The pitch size of the LED array is kept  $120\text{-}\mu\text{m}$  to minimize the cross talk between individual LED pixels. As seen from the single pixel, the indium bump is deposited on cathode and anode pads. Since we are observing light from the bottom side of the substrate, the complete mesa area is covered by a Ti/Au metal layer. A thick positive photo resist AZ 4620 of  $8\text{-}\mu\text{m}$  thickness is used for Indium metal deposition and liftoff process. For flip chip bonding we used Karl Suss FC150 flip chip bonding machines. After flip chip bonding, the GaSb substrate from the bottom side of the device is thinned by lapping and polishing. The final thickness of the GaSb substrate is measured by optical microscopy as well as by a Fourier transform infrared (FTIR) spectrometer and is found to be  $50\ \mu\text{m}$ .

In Fig. 4, we have shown the picture of LED array flip chip onto CMOS driver. Wire bonding is done between the bonding pads in CMOS array and the pads on the ceramic package. There are test LED devices at the four corners, which can be tested directly without going through the Si-CMOS driver circuits. These devices are used to measure the single LED performance as well as to monitor the flip chip bonding process. Besides four corner LED test pads, there are 296 bonding pads in the CMOS driver to bias each LED pixel independently. The array is mounted on an electronic driver board which supplies

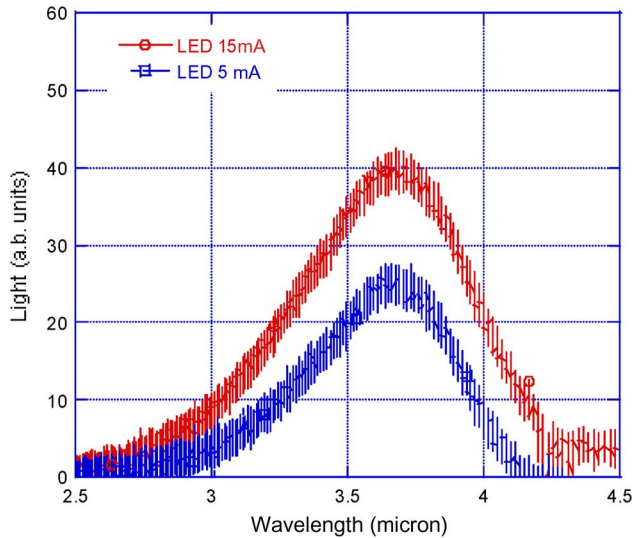


Fig. 5. MWIR LED spectra at two injection currents.

various biasing voltages, and the light output is measured by using a SBIR  $320 \times 256$  InSb focal plane array camera. We use a 2-in ZnSe lens to focus the LED picture onto the IR camera.

### III. RESULTS AND DISCUSSIONS

The spectra of light emission from LEDs are measured by the Fourier transform infrared (FTIR) spectroscopic technique. Fig. 5 shows the room temperature spectra of light emission from the LED device with 16 cascade layers with two injection current levels. The luminescence spectra of the device peak at  $3.8 \mu\text{m}$ . There is very little peak wavelength shift for injection currents of 5 and 15 mA. This may be due to the small difference in injection current levels.

We performed flip chip experiments varying bonding pressure between 3 and 11.5 Kg. We used a Karl Suss FC 150 flip chip bonding machine for flip chip experiments. The results of the bonding experiments in the FC 150 machine are shown in Fig. 6. First for optimization experiments, we used a test chip array with only metal pads and two indium bumps for each pixel. Similarly, we also use a test chip for the driver side with metal pad and indium bumps. We measured the continuity of bonding by measuring the resistance at two test pads on the driver side of the test chips. After the flip chip bonding, we pulled apart the test chips and then took a scanning electron microscope (SEM) picture of the pad area. We performed experiments with bonding at room temperature and  $100^\circ\text{C}$ . We also varied the bonding time between 60 to 300 s. This is the time for which the bonding pressure was applied. For  $100^\circ\text{C}$  bonding sample, forced air cooling was used to cool down to  $80^\circ\text{C}$  and then a normal cooling cycle was used.

As it is seen in Fig. 6(a) and (b), the bonding was done with 8.5-kg pressure either at room temperature or  $100^\circ\text{C}$  bonding temperature and 60-s bonding time. The SEM pictures show good contact and very low deformation of indium bumps. In case of the samples (c) and (d), the indium pads are deformed heavily and may result in shorts in large array. By comparing Fig. 6(a) and (b), the SEM picture shows similar deformation of the bonding pads and the spreading is acceptable. Since we

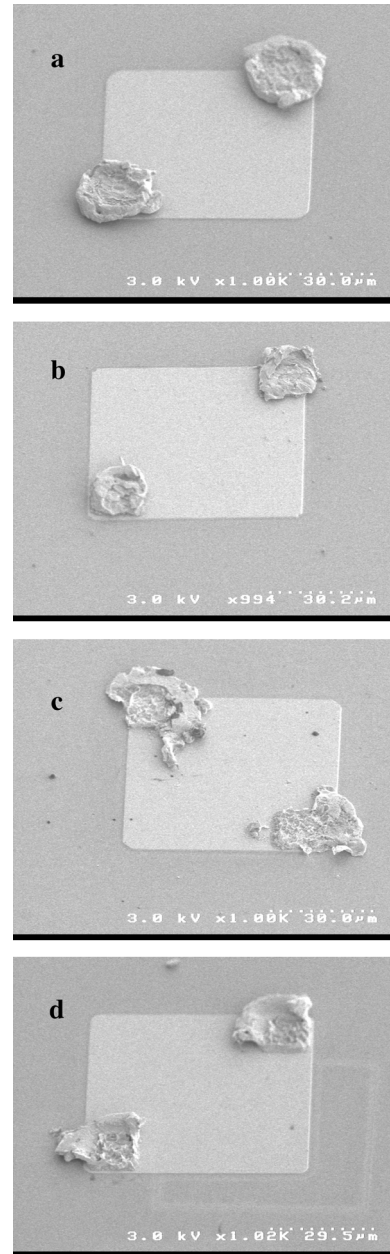


Fig. 6. SEM picture of indium bump with different flip chip conditions. (a) 8.5 Kg/RT/60 s. (b) 8.5 Kg/ $100^\circ\text{C}$ /60 s. (c) 8.5 Kg/ $100^\circ\text{C}$ /300 s. (d) 11.5 Kg/ $100^\circ\text{C}$ /60 s.

do not want the indium bump to be deformed due to high-temperature stress, we limit the bonding temperature much lower than Indium melting temperature ( $156.7^\circ\text{C}$ ). However, we have also done contact resistance measurement (not shown here) and found that sample (b) has lower resistance than sample (a). It may be due to fact that at higher temperature Indium oxide breaks down easily and hence causes low contact resistance. Hence, we used 8.5-kg pressure,  $100^\circ\text{C}$  bonding temperature, and 60 s bonding time for all the arrays the results of which is presented in this paper. The applied pressure is equivalent to approximately 1 g per bump which is higher than previously reported results [12]. This may be due to the fact that we have two bumps per pixel where the authors in the paper [12] have used single bump per pixel.

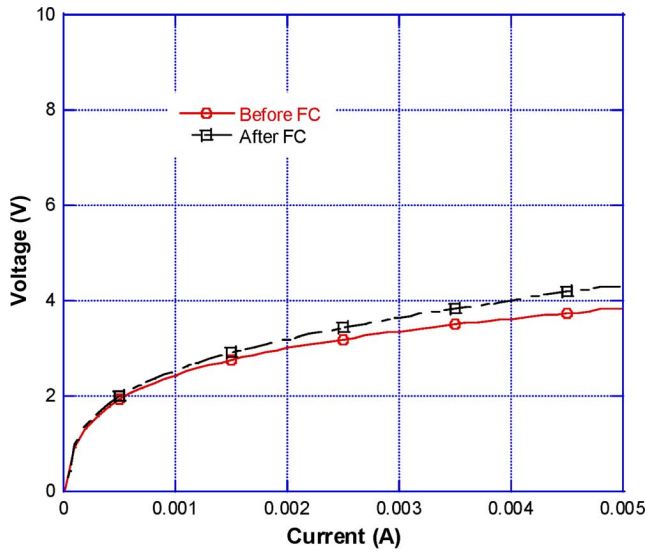


Fig. 7.  $I$ - $V$  curves for device before and after flip chip bonding.

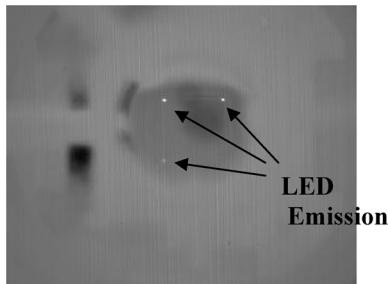


Fig. 8. Photograph of MWIR LED emission at three corners of the array.

We measured the current voltage ( $I$ - $V$ ) curves for devices before flip chip bonding and after flip chip bonding. The voltage drop is about 4 V at 5-mA injection current, which is typical for a 16-stage SLED structure. As seen in Fig. 7, the  $I$ - $V$  curves look similar which indicates that the resistance increase due to flip chip bonding is negligible. We observed very little increase in voltage drop in the device at low injection current levels. However, the voltage drop at higher injection current level is a little higher for flip chip devices. Though we have shown here results from two devices, we observed uniform IV curves from LED devices at four corners of the array. In an earlier paper [2], we have shown that the peak wavelength of emission shift to higher wavelength for higher injection current densities.

We used a Santa Barbara Infrared (SBIR)  $320 \times 256$  InSb focal plane array camera for observing the light emission from the LED array. The camera has a liquid nitrogen pour filled dewar and operates at 77 K. A ZnSe 2-in focal length lens is used to magnify the LED array while taking pictures using the IR camera. The array is mounted onto a 68-pin LCC package and kept in the dewar for biasing the devices. As seen in Fig. 8, LEDs at three corners of the  $68 \times 68$  array are emitting light. The LED at the fourth corner was not working before flip chip bonding, and hence we do not expect to see the light from this LED. From the light emission pictures, we concluded that the flip chip process results in good contact between CMOS driver and LED array.

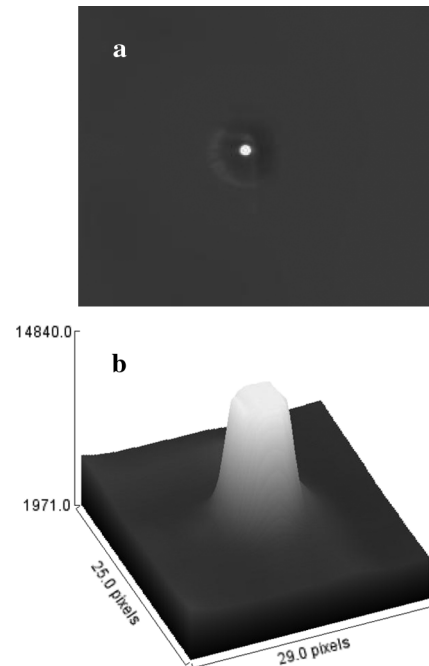


Fig. 9. (a) MWIR camera picture of single LED. (b) Surface plot of the light emission from single LED.



Fig. 10. Picture of light emission from full array.

We took a photograph of light emission from one of the corner LEDs of the array. We used a 1-in focal length ZnSe lens for this figure which is different from 2-in focal length lens used for Fig. 8. The injection current was 10 mA and the voltage drop across the device was 5.5 V. The background at the corner of the LED array is also seen in picture. We also took the surface plot of the light emission across the LED and have shown in Fig. 9(b). Though we expect the picture to be square, because of focus error the pixel looks circular. The light emission is quite uniform across the LED mesa area and also goes down to background level outside the mesa area.

In Fig. 10, we have shown the light emission from complete  $68 \times 68$  LED array. We have not tried to light the entire array because not all the wire-bonds for power pads are connected. Though we need approximately 290 pads for biasing the complete array, we have only 68 pins available from the LCC package. In a few cases, we have double the wire bonds from

LED array to each pad on LCC package. The picture shows very good contact across the array and approximately 90% of the LEDs in the array are emitting lights. It may be noted that few center rows/columns are not accessible due to number of available bonding pads, and they are seen dark for that reason.

#### IV. SUMMARY

The MWIR LED arrays were flip chip bonded onto a Si-CMOS driver array. Both the LED and CMOS driver arrays have indium bumps which were deposited by a thermal evaporation technique. We used a thermo-compression technique to flip chip bond the LED and CMOS driver arrays. On the basis of contact resistance and change in bump shape after flip-chip bonding the accurate bond pressure, time, and temperature are found to be 8.5 kg, 60 s, and 100 °C, respectively. The arrays are lapped and polished after flip chip bonding and before mounting on to the LCC package. The device electrical IV characteristics as well as optical emission characteristics were measured. Since we have two bumps per pixel (anode and cathode contacts) approximately 1 g per bump is required for flip chip bonding. Though we have presented the results from room-temperature measurements, we intend to carry out cryogenic testing of the LED arrays and expect the flip chip bonding process will not have any degrading effect on contact resistance. We have not tried a soldering reflow technique for flip chip bonding and hope similar experiments will be more rewarding.

#### ACKNOWLEDGMENT

The authors would like to thank S. Allison of Advanced Research Corporation (ARC) for help in flip chip bonding.

#### REFERENCES

- [1] D. B. Beasley *et al.*, "Dynamic IR scene projector based upon the digital micro mirror device," *Proc. SPIE*, vol. 4366, pp. 96–104, 2001.
- [2] N. C. Das and M. Tobin, "Performance of mid-wave infrared (3.8 mm) light emitting diode device," *Solid State Electron.*, vol. 50, pp. 1612–1617, 2006.
- [3] S. J. Chang, C. S. Chang, Y. K. Su, C. T. Lee, W. S. Chen, C. F. Shen, Y. P. Hsu, S. C. Shei, and H. M. Lo, "Nitride-based flip-chip ITO LEDs," *IEEE Trans. Adv. Packag.*, vol. 28, no. 2, pp. 273–277, May 2005.
- [4] J. R. Le, S. L. Na, J. H. Jeong, S. N. Lee, J. S. Jang, S. H. Lee, J. J. Jung, J. O. Song, T. Y. Seong, and S. J. Park, "Low resistance and high reflectance Pt/Rh contacts to p-type GaN for GaN-based flip-chip light emitting diodes," *J. Electrochem. Soc.*, vol. 152, pp. G92–G94, 2005.
- [5] J. Song, D. S. Lee, J. S. Kwak, O. H. Nam, Y. Park, and T. Y. Seong, "Low resistance and reflective Mg-doped indium oxide-Ag ohmic contacts for flip-chip light emitting diodes," *IEEE Photon. Lett.*, vol. 16, no. 6, pp. 1450–1452, Jun. 2004.
- [6] J. L. Tissot, "Advanced IR detector technology development at CEA/LETI," *Infrared Phys. Technol.*, vol. 43, pp. 223–228, 2002.
- [7] J. P. Long, S. Varadarajan, J. Matthews, and J. F. Schetzina, "UV detectors and focal plane array imagers based on AlGaIn p-i-n photodiodes," *Opto-Electron. Rev.*, vol. 10, pp. 251–260, 2002.
- [8] M. Li *et al.*, "Smart structures devices and systems II," *Proc. SPIE*, vol. 5650, pp. 9–16, 2005.
- [9] R. McClintock, K. Mayes, A. Yasan, D. Shiell, P. Kung, and M. Razeghi, "320 × 256 solar-blind focal plane arrays based on AlxGa1-xN," *Appl. Phys. Lett.*, vol. 86, pp. 11117-1–11117-3, 2005.
- [10] S. J. Chang, W. S. Chen, Y. C. Lin, C. S. Chang, T. K. Ko, Y. P. Hsu, C. F. Shen, J. M. Tsai, and S. C. Shei, "Nitride based flip chip LEDs with transparent ohmic contacts and reflective mirrors," *IEEE Trans. Adv. Packag.*, vol. 29, no. 3, pp. 403–408, Aug. 2006.
- [11] N. C. Das, K. Olver, F. Towner, G. Simonis, and H. Shen, "Infrared (3.8 μm) interband cascade light-emitting diode array with record high efficiency," *Appl. Phys. Lett.*, vol. 87, pp. 41105-1–41105-3, 2005.
- [12] K. Chu, J. S. Lee, H. S. Cho, B. S. Rho, H. H. Park, and D. Y. Jeon, "Characteristic of Indium bump for flip chip bonding used in Polymeric waveguide Integrated optical interconnect systems," *Jpn J. Appl. Phys.*, vol. 43, pp. 5922–5927, 2004.



**Naresh Chandra Das** (SM'08) received the Ph.D. degree from Utkal University, Bhubaneswar, India, in 1986 and performed his thesis work at the Central Electronics Engineering Research Institute, Pilani, India.

Prior to joining the microphotonics branch at the Army Research Laboratory in 2000, he worked at the Indian Institute of Technology (IIT), Mumbai, Bharat Heavy Electricals, Ltd., Bangalore India, Kirtland Air Force Base, Albuquerque, NM, and NASA/GSFC, Greenbelt, MD. His current research areas are design, fabrication, and characterization of IR LEDs and lasers.



**Monica Taysing Lara** has been an Electronics Engineer with the U.S. Army Research Laboratory since 1986. She developed techniques for growing GaAs/AlGaAs superlattice and quantum well on GaAs substrates using the molecular beam epitaxy (MBE). In the area of processing of semiconductor devices, she helped to develop FETs, HEMTs, picoseconds switches, infrared detectors, optical modulators, waveguides, and VCSELs. She also characterized III and V quantum well material by photoluminescence and reflectance, and evaluated

the electrical characteristics of devices. Currently, she is working on photonics bandgap crystal (PBG) structures.



**Kimberley Anderson Olver** received the B.A. degree in chemistry/biochemistry from Goucher College, Towson, MD, in 1981.

She is currently the packaging lead for the Electro Optics and Infrared Materials Branch at the Army Research Laboratory, Adelphi, MD. Prior to working for the Army Research Laboratory, she was a Senior Engineer with the Advanced Infrared Technology Department, Lockheed Martin Laboratories (formerly Martin Marietta Laboratories), Baltimore, MD, where her work included characterization and

packaging of IR detectors and FPAs. Her previous work experience has also included extensive materials research, as well as surface and failure analysis utilizing Auger, XPS, and SIMS.

**Fouad Kiamilev**, photograph and biography not available at the time of publication.

**J. P. Prineas**, photograph and biography not available at the time of publication.

**J. T. Olesberg**, photograph and biography not available at the time of publication.

**E. J. Koerperick**, photograph and biography not available at the time of publication.

**L. M. Murray**, photograph and biography not available at the time of publication.

**Tom F. Boggess** photograph and biography not available at the time of publication.